PIV Measurements of Airflow and Ink Mist Motion around Ink Jet Nozzles

Nobuyuki Hirooka, Yoshihiko Ono, Kazuhiro Mori** and Nobuyuki Nakayama*
Research & Development Center
**Ink Jet Business Group*
***Product Verification Center, Customer Focus & Quality Unit*
Fuji Xerox Co., Ltd.
Kanagawa, Japan

Abstract

Dispersed ink mist occurs around ink jet nozzles and contaminates the inside of a thermal ink jet printer. It is required to clarify the fine droplet motion in order to prevent the contamination effectively. First, ink mist was visualized and airflow around ink jet nozzles was measured by Particle Image Velocimetry (PIV), when an ink jet carriage was scanned. Dispersed ink mist was observed at an upstream side of nozzles in scan direction, and it was confirmed that ink mist was blown up by the airflow. In addition, it was clarified that the airflow between a carriage and a paper varied depending on the carriage speed. Secondly, fundamental characteristics of ink droplets in the vicinity of ink jet nozzles were measured. The results reveal that PIV measurement is effective to gain an understanding of ink jet performance. Finally, airflow around ink jet nozzles was calculated numerically by Computational Fluid Dynamics (CFD). The results agree qualitatively with the experiments. Valuable design information to reduce mist contamination was obtained by the investigation.

Introduction

Ink jet printers are of worldwide general use, and high performance has been required. Recently, the printers have been improved highly in quality and speed. Whereas, dispersed mist, which is minuscule ink droplets and does not land in a recording media, occurs noticeably inside a printer. It contaminates the inside and affects adversely the machine control. It is very important to prevent the contamination effectively and achieve high-quality imaging. Therefore, direct observation and quantitative measurement on ink mist motion have been expected. Images of dispersed ink mist between a printhead and a recording media have captured and the phenomenon has been directly confirmed[1] so far. However, ink mist and airflow between them have not been measured quantitatively. It has been relatively difficult measurement because ink mist and airflow move fast in a narrow gap. In place of experimental studies, numerical studies have been performed. In numerical simulation, ink droplet motion between a carriage and a recording media has been predicted by Computational Fluid Dynamics (CFD). It was reported that vortex-like flow was generated by the interaction of ink droplets and flow field through momentum exchange.[1]

In this study, Particle Image Velocimetry (PIV) was applied to visualize dispersed ink mist motion and measure quantitatively velocity distributions of ink mist and airflow. Moreover, ink droplets in the vicinity of ink jet nozzles were measured to gain an understanding of the fundamental characteristics and ink jet performance. PIV is a powerful technique for visualization and quantitative measurement on fluid field and powder dynamics. The measurement results were discussed by comparison with the results calculated by FLUENT Ver.5.5 (Fluent Inc., Lebanon, NH, U.S.A).

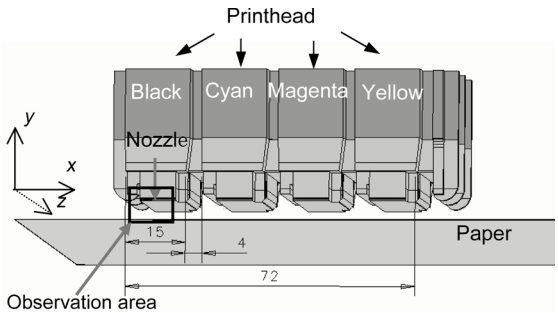

Figure 1. Ink jet carriage

Measurement Method

A ink jet carriage is described schematically in Fig. 1. Printheads of Black, Cyan, Magenta and Yellow ink are arranged in a line flatly. Observation area is around black ink nozzles because the black ink forms a striking. The nozzles for ejecting black ink are arranged herein (area in *z*-direction: 2.54 mm, total number of nozzles: 832). The carriage speed was controlled at 0.57 m/s and 1.14 m/s,

respectively. Jetting frequency was 9 kHz at 0.57 m/s and 18 kHz at 1.14 m/s. The carriage is set against a recording media with a narrow space (approximately 1.7 mm). The space may fluctuate slightly due to setting condition.

The PIV system used in the experiment for ink mist and airflow is described schematically in Fig. 2. A doublepulsed Nd:YAG laser (New Wave Research, Inc., Solo-III, wavelength: 532 nm, maximum energy: 50 mJ/pulse) was used to supply the pulsed laser sheet and illuminate observation area at intervals of 70-140 μs. Thickness of laser sheet was 7 mm for mist visualization and 0.29 mm for the others. Images were captured through zoom lens (Keyence Corporation, VH-Z05, depth of field: 2.3 mm) and a CCD camera (Hamamatsu Photonics K.K., C7300, 1280×1024 pixels, 12 bit). In order to analyze a pair of images, the pattern tracking algorithms was used.[2] The resolution of a captured image was 8.18 μm/pixel. The interrogation window was defined 35 pixels. Smoke of incense stick was used for tracing particles.

The PIV system used in the experiment for ink droplets motion in the vicinity of nozzles is described schematically in Fig. 3. The experimental system consists of a printhead, driving unit for ejecting ink droplets, aforementioned PIV system and ancillary apparatus like a filter and a beam splitter. A filter and a beam splitter were used for intensity reduction. A double-pulsed Nd:YAG laser was illuminated at interval of 1 μs. The resolution of a captured image was 0.43 μm/pixel. The captured images were analyzed by commercially available software.

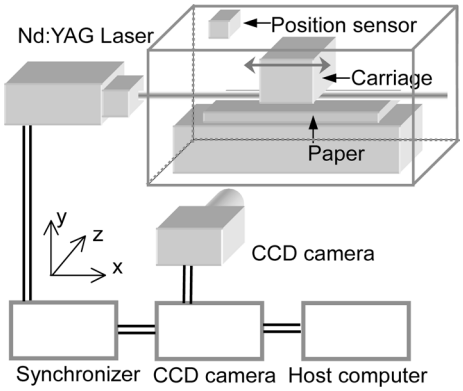

Figure 2. Experimental setup for ink mist and airflow

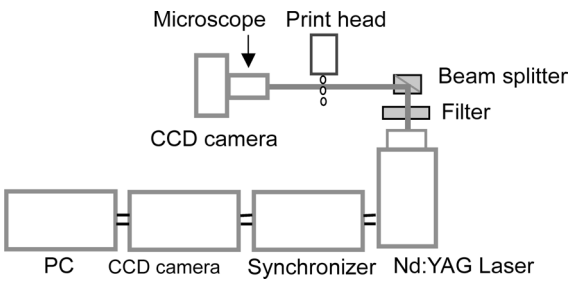

Figure 3. Experimental setup for ink droplet motion

Experimental Result

Visualization of Ink Mist Motion

In order to investigate fundamental characteristics of ink mist motion, ink mist around nozzles was visualized. Examples of captured images, when black ink droplets were ejected and a carriage was scanned, are shown in Fig. 4. Scan speed of the carriage was 0.57 m/s in Fig. 4 (a), and 1.14 m/s in Fig. 4 (b). The figures show that the thick white line from the nozzle to the paper indicates main droplets to move toward the paper, and the numerous white spots spreading toward upstream side in scan direction are ink mist. At scan speed 0.57 m/s, ink mist remains close to the paper, and at the speed 1.14 m/s, it floats apart from the paper. We confirmed that ink mist was extensively present in upstream side of a nozzle. In addition, comparison of Fig. 4 (a) and (b) reveals that the distribution of ink mist shifts according to the magnitude of scan speed.

Distributions of mean luminance between the point A and B (ref. Fig. 4 (a)) were measured along the *y*-axis from the printhead to the paper. The distributions along the *y*-position are shown in Fig. 5. The figure shows that there are two extremal values per a dotted line: one indicates the position of the paper, and the other indicates the center of the ink mist distribution. At the horizontal axis, the nozzle positions correspond approximately to 240 pixel. The figure shows that ink mist exists in large numbers close to the paper at scan speed 0.57 m/s, and it moves upwards approximately 40 pixels at 1.14 m/s. The difference in the ink mist distribution is thought to correspond to the difference in the scan speed and the velocity of the airflow around nozzles.

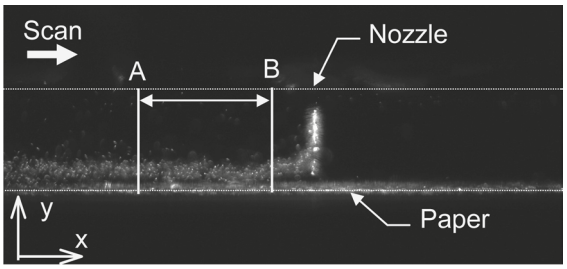

(a) Scan speed 0.57 m/s

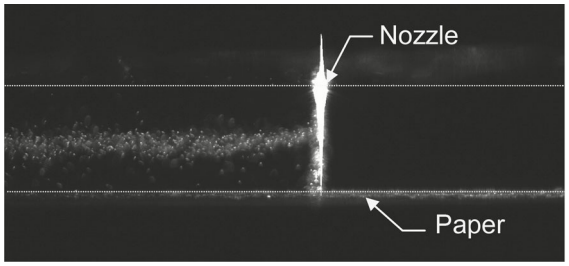

(b) Scan speed 1.14 m/s

Figure 4. Ink mist visualized around nozzles

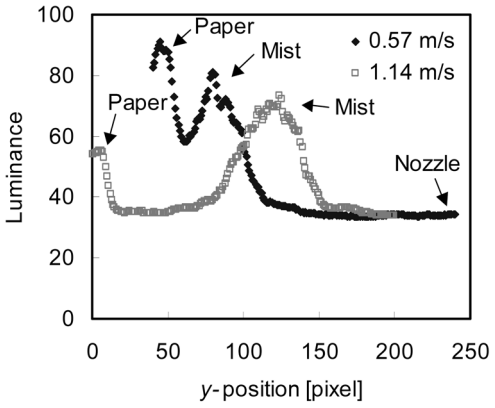

Figure 5. Distribution of mean luminance

Measurement of Airflow

Airflow between a carriage and a recording media, which influenced ink mist motion, was measured quantitatively by PIV. An example of captured images, when a carriage was scanned at 1.14 m/s and black ink droplets were ejected, are shown in Fig. 6. Velocity vectors are plotted in Fig. 7. Figure 7 (a) and (b) show instantaneous velocity vectors at scan speed 0.57 m/s and 1.14 m/s, respectively. The flow field described in each figure corresponds to the rectangular frame drawn in Fig. 6. It is of great concern that vortex-like flow is formed at the upstream side of the nozzles in scan direction. At scan speed 0.57 m/s, the center of the vortexlike flow is approximately in the intermediate position between the printhead and the paper. At scan speed 1.14 m/s, it moves toward the printhead side. It compares well with the ink mist distribution. Ink droplets ejected to the paper form the stream toward the paper, and the airflow spreads upward around the paper. The spread airflow flows with the airflow around the printhead.

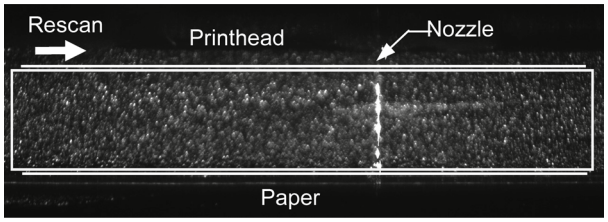

Figure 6. Tracing particle image (scan speed 1.14 m/s)

Velocity distributions of the airflow and the ink mist in *x*-direction are shown in Fig. 8. The position in *y*-direction is 1.2 mm and 0.9 mm from the printhead, respectively. Nozzle positions correspond approximately to the position 700 pixel at the horizontal axis. The figure shows that the velocity of ink mist agrees approximately with the velocity of the airflow. Comparison of the velocity of the airflow and the ink mist reveals that ink mist is flowed by airflow around nozzles. Since ink mist move faster toward upstream side of nozzles due to the increase in scan speed, amount of ink mist is thought to increase with increasing scan speed.

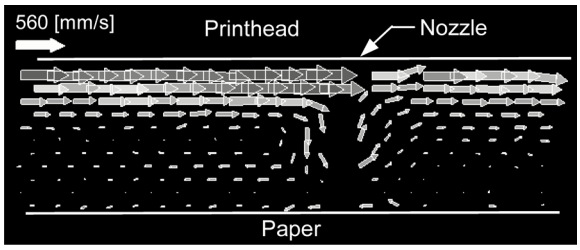

(a) Scan speed 0.57 m/s

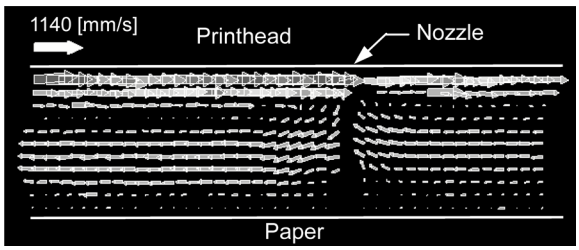

(b) Scan speed 1.14 m/s

Figure 7. Velocity vectors between a printhead and a paper

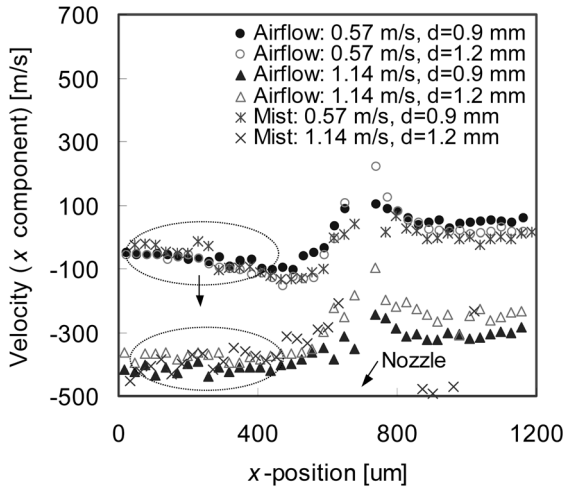

Figure 8. Velocity profiles at the x-position

Measurement of Ink Droplet Motion

Ink droplets in the vicinity of nozzles, just after the time when they are ejected, are shown in Fig. 9. Figure 9 (a) shows a pair of images, frame interval of the images is 1 μs, at 40μs after the ejection, and Fig. 9 (b) at 70μs, and Fig. 9 (c) at 90μs. The size of ink droplets was confirmed to be smaller as time goes by. We call this kind of ink droplets captured mainly in Fig. 9 (a) "main ink droplet", in Fig.9 (b) "satellite ink droplet" and in Fig.9 (c) "follower ink droplet". The general ejection process of ink droplets is as follows:

1. Main ink droplets are ejected and move toward a recording media.
2. Elongated ink droplets formed at the end of main ink droplets are divided into several ink droplets, which are follower ink droplets.
3. Follower ink droplets are ejected at last in the process.

We note the salient third process, because follower ink droplets are subject to be ink mist.

Distributions of size and velocity of ink droplets, shown in Fig. 9 (a)-(c), were investigated, respectively. Distribution of ink droplet size at the *y*-position is shown in Fig. 10. The vertical axis is ink droplet diameter obtained based on an image analyzed by an image processor. The mean diameters of the main, satellite and follower ink droplets were approximately 28 μm, 12μm and 6μm, respectively. Distribution of ink droplet velocity at the *y*-position is shown in Fig. 11. The vertical axis is ink droplet velocity analyzed by an image processor employed particle tracking algorithm. The mean velocity of the main, satellite and follower ink droplets was approximately 12 m/s, 8 m/s and 5 m/s, respectively. Follower droplets are relatively smaller size and slower velocity, therefore it is thought that they are flowed by the air flow around nozzles.

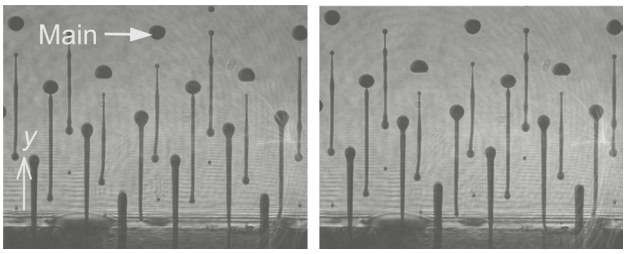

(a) 40 μs after the start of ejecting

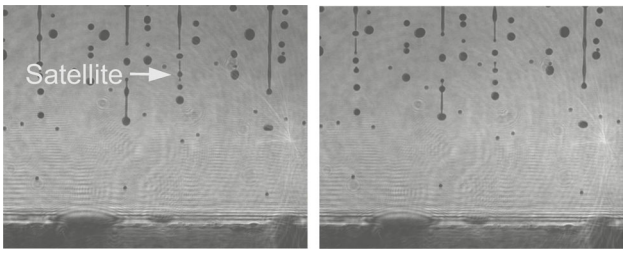

(b) 70 μs after the start of ejecting

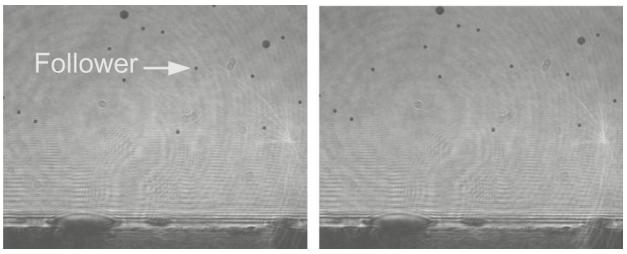

(c) 90 μs after the start of ejecting

Figure 9. Images of ink droplets in the vicinity of nozzles

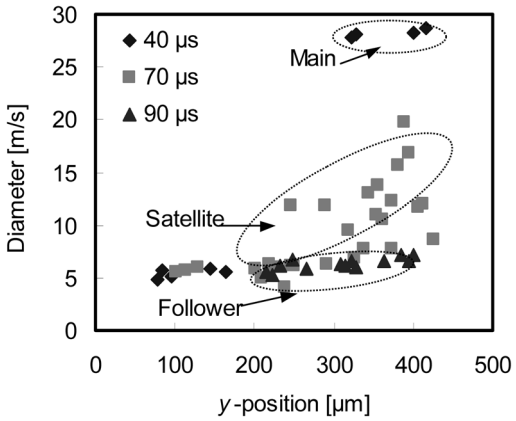

Figure 10. Distribution of ink droplet size

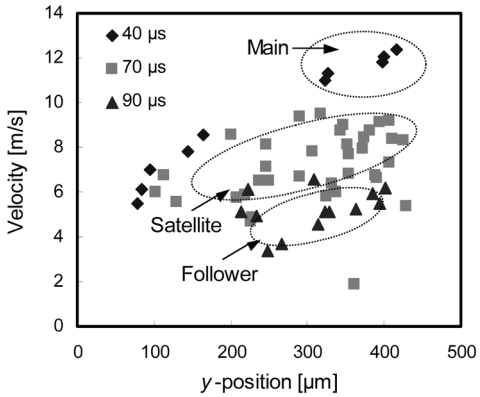

Figure 11. Distribution of ink droplet velocity

Numerical Simulation

Numerical Method

In order to verify the accuracy of numerical results, the velocity distributions described in Fig. 7 were compared to the numerically calculated results.

FLUENT[3] was used to solve Navier-Stokes equations numerically:

$$\frac{\partial \rho}{\partial t} + \frac{\partial \rho u_j}{\partial x_j} = 0 , \quad (1)$$

$$\frac{\partial \rho u_i}{\partial t} + \frac{\partial \rho u_i u_j}{\partial x_j} = \frac{\partial p}{\partial x_i} + \frac{\partial}{\partial x_j}\left(\mu \frac{\partial u_i}{\partial x_j}\right) + \rho g_i , \quad (2)$$

where ρ is the fluid density, p is the static pressure, and x_i (i=1,2,3) represent the Cartesian coordinates. u_i (i=1,2,3) represent the Cartesian components of velocity u, gi (i=1,2,3) the Cartesian components of gravitational acceleration g and μ the molecular viscosity of the fluid. The Einstein convention was adopted. It is reasonable to assume the fluid is incompressible for this problem.

FLUENT predicts the trajectory of a discrete phase particle by integrating the balance for the particle, which is written in a Lagrangian reference frame. This force balance equates the particle inertia with the forces acting on the particle, and can be written as

$$\frac{d\vec{u}_p}{dt} = F_D(\vec{u} \quad \vec{u}_p) + \frac{\rho_p \quad \rho}{\rho_p}\vec{g} + \vec{F}, \tag{3}$$

$$F_D = \frac{18\mu}{\rho_p D_p^2}\frac{C_D R_e}{24}. \tag{4}$$

The first term in the right hand side of Eq. (3) is drag force per unit particle, the second term is buoyancy and the third term is additional forces. Additional forces contain the virtual mass force, or force excited due to the pressure gradient. The third term F is ignored because droplet density is much greater than air density in this analysis. Here, u_p is the particle velocity, ρ_p is the density of the particle, and D_p is the particle diameter. *Re* is the relative Reynolds number and *CD* is the drag coefficient.

Analysis model, which has approximately 2 million cells, is shown in Fig. 12. It consists of a rectangular prism, 191 mm in length, with 84 × 155 in cross-sectional dimensions. The carriage size is 85.5 mm in length, 53.5 in width and 82.1 mm in height. The distance between the carriage and the paper is 1.9 mm. Since the carriage is static, the flow field and paper motion is inversely considered. Therefore, analysis was conducted at the moving coordinate system with the constant velocity. The velocity is prescribed at the inlet boundary and the pressure, which means static gauge pressure, is prescribed as 0 at the outlet boundary. The paper is modeled as a no slip wall at constant velocity and the other three surfaces are free-slip walls.

Ink droplets consist of one main droplet, five satellite droplets and one follower droplet per a nozzle. The initial velocity of a main droplet, satellite droplets and a follower droplet are 12 m/s, 8 m/s and 5 m/s, respectively, using characteristics of black ink ejection mentioned before. The volume density of ink droplet is 1050 kg/m^3, and 94 out of 832 nozzles are used. Ejecting frequency is 9 kHz at scan speed 0.57 m/s, and 18 kHz at 1.14 m/s.

Numerical Result

Figure 13 shows the velocity distributions of airflow around nozzles, obtained via calculated results at scan speed 0.57 m/s and 1.14 m/s, respectively. Velocity vectors were transformed to the fixed coordinate system. The length of velocity vectors is in proportion to velocity magnitude. The maximum velocity of the airflow is 0.84 m/s at scan speed 0.57 m/s, and 1.58 m/s at 1.14 m/s.

Vortex-like flow is formed at the upstream side of nozzles in scan direction, and the air at the downstream side is flowed toward the same direction with the scan. It indicates that numerical results agree qualitatively with experimental results. The measurement results indicate that the center of the vortex-like flow moves toward a printhead side at scan speed 1.14 m/s. However, numerical results indicate that it does not vary in scan speed. The difference between measurements and numerical results is thought to correspond to the difference in the detailed carriage design.

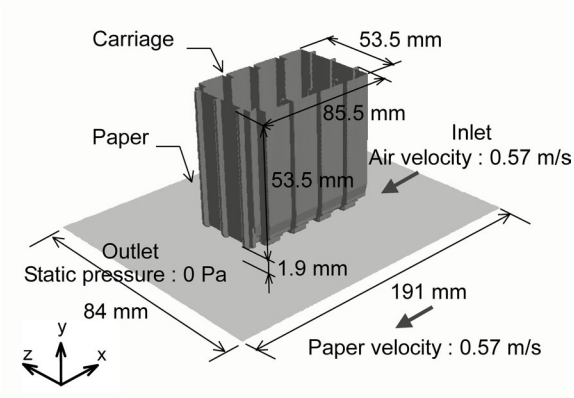

Figure 12. Analysis model

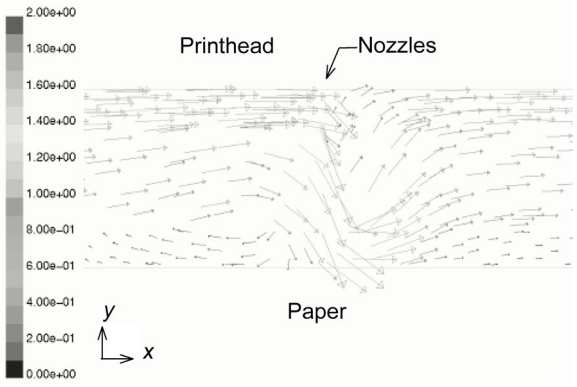

(a) Scan speed 0.57 m/s

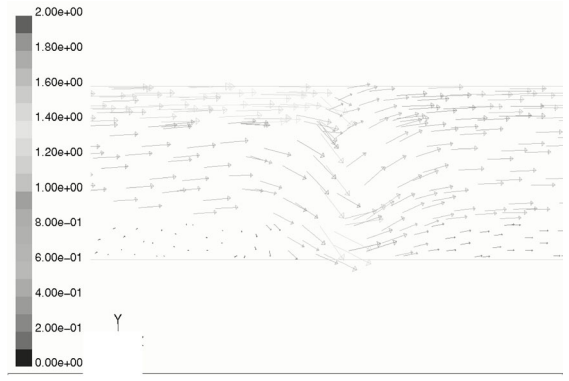

(b) Scan speed 1.14 m/s

Figure 13. Velocity vectors between the printhead and the paper

Conclusion

Particle Image Velocimetry (PIV) was applied to visualize and measure quantitatively dispersed ink mist motion and airflow around nozzles. In addition, fundamental characteristics, including ink mist size and ink mist velocity, were measured. The measurement results were discussed by comparison with the results calculated by CFD. The investigation clarified the following:

(1) Ink mist extensively remains at the upstream side of the nozzles in scan direction. Ink mist exists in large numbers close to the paper at scan speed 0.57 m/s, and it moves upwards at 1.14 m/s.

(2) Vortex-like flow is formed at the upstream side of nozzles. The center is in the intermediate position between the printhead and the paper at 0.57 m/s, and it moves toward the printhead side at 1.14 m/s. It compares well with the ink mist distribution.

(3) The velocity distribution of airflow corresponds approximately with that of ink mist. Ink mist follows the airflow.

(4) The mean diameters of the main, satellite and follower ink droplets are 28 μm, 12μm and 6μm, respectively. The mean velocity of them is 12 m/s, 8 m/s and 5 m/s, respectively.

(5) Numerical results agree qualitatively with experiments.

References

1. K. Mori, Computational Fluid Dynamics of Dispersed Mist Phenomenon in a Thermal Ink Jet Printer, J. Imaging. Sci. Technol., Vol. 47, No. 3, pp. 249-254. (2003).
2. A. Kaga, Y. Inoue, K. Yamaguchi, Pattern Tracking Algorithms for Airflow Measurement Through Digital Image Processing of Visualized Images, Journal of the Visualization Society of Japan, Vol.14, No.53, pp. 38-45. (1994)
3. Fluent Inc., FLUENT 5 User's Guide Vol. 3, Chap. 14 (1998).

Biography

Nobuyuki Hirooka received his MSc (Eng) degree in Mechanical Engineering from Meiji University (1998). In 1998, he joined Fuji Xerox Co., Ltd., where he has been engaged in research on electrophotography. He is currently working on numerical simulation and measurement of powder dynamics in electrophotography. He is a member of the Japan Society of Mechanical Engineering.